

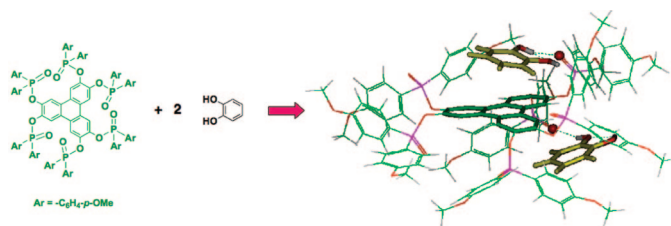
## Polyphosphorylated Triphenylenes: Synthesis, Crystal Structure, and Selective Catechol Recognition

Cécile Givelet,<sup>†</sup> Bernard Tinant,<sup>‡</sup> Luc Van Meervelt,<sup>§</sup> Thierry Buffeteau,<sup>†</sup>  
Nathalie Marchand-Geneste,<sup>†</sup> and Brigitte Bibal<sup>\*,†</sup>

Université de Bordeaux, Institut des Sciences Moléculaires, CNRS UMR 5255, 351 cours de la Libération,  
33405 Talence, France

b.bibal@ism.u-bordeaux1.fr

Received September 12, 2008



Designed as a multivalent hydrogen bond acceptor, new receptors, *Discopus* **1a,b**, were built from a triphenylene core surrounded by six (diaryl)phosphinate groups. An efficient synthesis was developed to prepare these elaborated structures in a high overall yield. The X-ray structure of receptor **1b** showed strong cooperative hydrogen bonds with two water molecules and intermolecular CH– $\pi$  contacts. In chloroform, *Discopus* **1a,b** displayed recognition properties toward dihydroxybenzenes, selectively forming complexes with catechol derivatives **4a–c** in a 1:2 (host:guest) stoichiometry. According to NMR and microcalorimetry titrations, association constants were found in the 30–2837 M<sup>-1</sup> range, which were larger than those reported for curvated catechol receptors (14–120 M<sup>-1</sup>). Interestingly, *Discopus* present two distinct catechol binding sites. Weak hydrogen bonding between host phosphinates and guest hydroxyl groups was shown by infrared spectroscopy and <sup>31</sup>P NMR. Molecular dynamics simulations and recognition experiments suggested that a stronger hydrogen bond assisted by a  $\pi$ -interaction between the *Discopus* core and one catechol molecule could exist within the 1:2 complex.

### Introduction

In molecular recognition, neutral polar P<sup>(V)</sup>=O groups are well-known for accepting hydrogen bonds, mainly forming complexes with ammoniums and metallic cations.<sup>1</sup> To improve weak P=O associations, multiple phosphoryl functions (phosphonate, phosphinate, and phosphine oxide) were largely introduced in macrocycles, clips, and cavitands to take advantages of preorganization and cooperativity.<sup>2</sup> In particular, polyphosphorylated resorcin[4]arenes successfully recognized

ammoniums in the gas phase,<sup>3</sup> solution,<sup>4</sup> and solid state.<sup>5</sup> Tetraphosphonated receptors were also efficient metallic cations extractors,<sup>6</sup> and di- or monophosphonated cavitands selectively detected alcohols and amines in the gas phase.<sup>7</sup> In these cases,

(2) (a) Caminade, A.-M.; Majoral, J.-P. *Chem. Rev.* **1994**, *94*, 1183–1213. (b) Schrader, T. *J. Inclusion Phenom. Mol. Recognit. Chem.* **1999**, *34*, 117–129. (c) Cherenok, S.; Dutasta, J.-P.; Kalchenko, V. *Curr. Org. Chem.* **2006**, *10*, 2307–2331. (d) Mlynarz, P.; Ruzinska, E.; Berlicki, L.; Kafarski, P. *Curr. Org. Chem.* **2007**, *11*, 1593–1609. (e) Dutasta, J.-P. *Top. Curr. Chem.* **2004**, *232*, 55–91.

(3) Gaz phase (a) Irico, A.; Vincenti, M.; Dalcanale, E. *Chem. Eur. J.* **2001**, *7*, 2034–2042. (b) Kalenius, E.; Moiani, D.; Dalcanale, E.; Vainiotalo, P. *Chem. Commun.* **2007**, 3865–3867.

(4) Liquid: (a) Lippman, T.; Wilde, H.; Dalcanale, E.; Mavilla, L.; Mann, G.; Heyer, U. *J. Org. Chem.* **1995**, *60*, 235–242. (b) Delangle, P.; Dutasta, J.-P. *Tetrahedron Lett.* **1995**, *36*, 9325–9328. (c) Biavardi, E.; Battistini, G.; Montalti, M.; Yebeutchou, R. M.; Prodi, L.; Dalcanale, E. *Chem. Commun.* **2008**, 1638–1640.

(5) Solid state: (a) De Zorzi, R.; Dubessy, B.; Mulatier, J.-C.; Geremia, S.; Randaccio, L.; Dutasta, J.-P. *J. Org. Chem.* **2007**, *72*, 4528–4531.

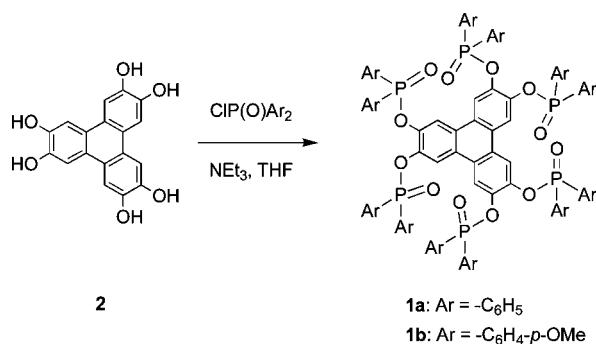
(6) (a) Delangle, P.; Mulatier, J.-C.; Tinant, B.; Declercq, J.-P.; Dutasta, J.-P. *Eur. J. Org. Chem.* **2001**, *19*, 3695–3704. (b) Bibal, B.; Tinant, B.; Declercq, J.-P.; Dutasta, J.-P. *Supramol. Chem.* **2003**, *15*, 25–32.

<sup>†</sup> Université de Bordeaux.

<sup>‡</sup> Université Catholique de Louvain, Laboratoire de cristallographie, Unité CSTR, 1, Place Pasteur, B-1348 Louvain-La-Neuve, Belgium.

<sup>§</sup> Department of Chemistry, Katholieke Universiteit Leuven, Celestijnenlaan 200F, B-3001 Leuven, Belgium.

(1) (a) Corbridge, D. E. C. *Phosphorus, an Outline of Its Chemistry, Biochemistry and Technology*, 4th ed.; Elsevier: Amsterdam, 1990; Chapter 14.1. (b) Kaplan, L. J.; Weisman, G. R.; Cram, D. J. *J. Org. Chem.* **1979**, *44*, 2226–2233. (c) Savage, P. B.; Holmgren, S. K.; Gellman, S. H. *J. Am. Chem. Soc.* **1993**, *115*, 7900–7901. (d) Savage, P. B.; Holmgren, S. K.; Gellman, S. H. *J. Am. Chem. Soc.* **1994**, *116*, 4069–4070.

SCHEME 1. Molecular Structure and Synthesis of *Discopus* 1a,b

receptors abilities benefit from partial or total guests encapsulation into host hydrophobic cavities. Few examples of hydrogen bonding between neutral species and mono- or polyphosphorylated receptors in solution have been reported.<sup>8</sup>

As natural and estrogenic (multi)phenols are attractive targets,<sup>9</sup> we were interested in new hydrogen bond acceptor architectures. To investigate such aromatic targets, our strategy was to combine several phosphinate patterns with a polyaromatic core. Indeed, polyaromatic compounds are attractive building blocks, combining synthetic and structural advantages: easy preparation, low-cost material, poly peripheral substituted positions, hindered regions, and potential  $\pi$ -interaction as well as photophysical properties. 2,3,6,7,10,11-Hexasubstituted triphenylenes were the ideal candidates to evaluate polyphosphorylated substituents in terms of cooperative and selective binding.

We designed *Discopus* 1a,b as new unpreorganized structures displaying a nanosized discotic surface (*Disco*) with six peripheral substituents (Scheme 1). This bulky phosphinate outside rim (*pus*) can prevent core self-aggregation and favor H-bonding. To the best of our knowledge, this is the first time that neutral phosphoryl groups are incorporated to a non-curved or non-macrocyclic architecture for recognition purpose.<sup>10,11</sup>

Herein this paper presents *Discopus* 1a,b synthesis from triphenylene 2 and their binding properties toward aromatic targets and aromatic hydrogen bond donor guests 4 (Figure 1). To evaluate

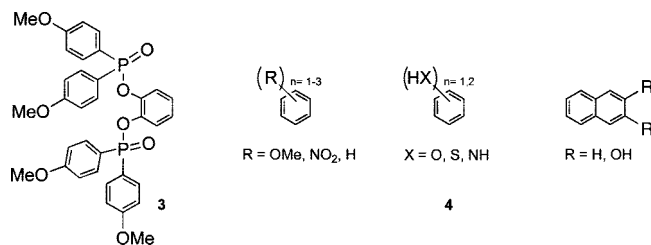


FIGURE 1. Model receptor 3 and aromatic targets 4.

core participation and multivalency effects, a simpler compound, 1,2-bis(diaryldiethylphosphinate)benzene 3, will be studied as a model receptor and compared to *Discopus* binding abilities (Figure 1).

## Results and Discussion

**Synthesis.** 2,3,6,7,10,11-Hexahydroxytriphenylene 2 was synthesized using a two-step procedure<sup>12</sup> in 77% overall yield. Hexaphosphorylation of compound 2 was then achieved in anhydrous conditions using commercial chloro(diphenyl)phosphine oxide or freshly prepared chloro-di(*p*-methoxybenzene)-phosphine oxide<sup>13</sup> in the presence of triethylamine in THF (Scheme 1). After workup, pure compounds 1a and 1b were isolated in 63% and 61% yield, respectively. *Discopus* 1a was soluble only in chlorinated solvents, whereas *Discopus* 1b was soluble in most common organic solvents. Both <sup>1</sup>H NMR spectra were characteristic of hexasubstituted triphenylenes, displaying a single signal for core aromatic protons.<sup>14</sup> <sup>31</sup>P NMR analysis also revealed that the six diaryldiethylphosphinate groups are equivalent (singlet at  $\delta_{31P}$  (CDCl<sub>3</sub>) 32.53 ppm for 1a and 33.28 ppm for 1b). The absorption spectra of both compounds in chloroform showed a maximum at 274 nm (see Supporting Information), which was comparable to the behavior of hexa(*n*-alkyloxy)-triphenylenes<sup>15</sup> in chlorinated solvents. Elaborated structures 1a,b were thus consistent with classical hexasubstituted triphenylenes. The same synthetic procedure was successfully used for the preparation of model 3 (60% yield from catechol).

**X-ray Analysis.**<sup>16</sup> Single crystals suitable for X-ray analysis of *Discopus* 1b were grown from the slow evaporation of a *n*-pentane/diethylether solution. The stoichiometry observed in the crystal structure is 1b·Et<sub>2</sub>O·2H<sub>2</sub>O with one-half of the complex in the asymmetric part of the unit cell (Figure 2). The deviation from the best mean plane through the eighteen core carbon atoms is only 0.021 Å, showing that the polyaromatic core is not distorted by the bulky substituents (Figure 2a). Bonds P1=O and P2=O are located under the core plane and make an angle of, respectively, 1.64° and 1.73° with this plane,

(7) Pinalli, R.; Nachtigall, F. F.; Ugozzoli, F.; Dalcanale, E. *Angew. Chem., Int. Ed.* **1999**, *38*, 2377–2380. (c) Pinalli, R.; Suman, M.; Dalcanale, E. *Eur. J. Org. Chem.* **2004**, *22*, 451–462. (d) Pirondini, L.; Dalcanale, E. *Chem. Soc. Rev.* **2007**, *36*, 695–706.

(8) (a) Segura, M.; Bricoli, B.; Casnati, A.; Muñoz, E. M.; Sansone, F.; Ungaro, R.; Vincent, C. *J. Org. Chem.* **2003**, *68*, 6296–6303. (b) Friedrichsen, B. P.; Whitlock, H. W. *J. Am. Chem. Soc.* **1989**, *111*, 9132–9134. (c) Friedrichsen, B. P.; Whitlock, H. W. *J. Am. Chem. Soc.* **1990**, *112*, 8931–8941.

(9) (a) Wiskur, S. L.; Anslyn, E. V. *J. Am. Chem. Soc.* **2001**, *123*, 10109–10110. (b) ten Cate, M. G.; Reinhoudt, D. N.; Crego-Calama, M. *J. Org. Chem.* **2005**, *70*, 8443–8453. (c) Preziosi, P. *Pure Appl. Chem.* **1998**, *70*, 1617–1631.

(10) Substituted (metallo)porphyrins analogues as flat molecular receptors: (a) Ogoshi, H.; Mizutani, T.; Hayashi, T.; Kuroda, Y. In *The Porphyrin Handbook*; Kadish, K. M., Smith, K. M., Guillard, R., Eds.; Academic Press: New York, 2000; Vol. 6, pp 279–340. (b) Weiss, J. *J. Inclusion Phenom. Macrocyclic Chem.* **2001**, *40*, 1–22, and references therein. (c) Sessler, J. L.; Camiolo, S.; Gale, P. A. *Coord. Chem. Rev.* **2003**, *240*, 17–55. (d) Even, P.; Boitrel, P. *Coord. Chem. Rev.* **2006**, *250*, 519–541.

(11) Triphenylene-based receptors: (a) O'Leary, B. M.; Grotzfeld, R. M.; Rebek, J., Jr. *J. Am. Chem. Soc.* **1997**, *119*, 11701–11702. (b) Waldvogel, S. R.; Wartini, A. R.; Rasmussen, P. H.; Rebek, J. *Tetrahedron Lett.* **1999**, *40*, 3515–3518. (c) Waldvogel, S. R.; Fröhlich, R.; Schalley, C. A. *Angew. Chem., Int. Ed.* **2000**, *39*, 2472–2475. (d) Schopohl, M. C.; Siering, C.; Kataeva, O.; Waldvogel, S. R. *Angew. Chem., Int. Ed.* **2003**, *42*, 2620–2623. (e) Bomkamp, M.; Siering, C.; Landrock, K.; Stephan, H.; Fröhlich, R.; Waldvogel, S. R. *Chem. Eur. J.* **2007**, *13*, 3724–3732, and references therein. (f) Fyfe, M. C. T.; Lowe, J. N.; Stoddart, J. F.; Williams, D. J. *Org. Lett.* **2000**, *2*, 1221–1224. (g) Badjic, J. D.; Cantrill, S. J.; Stoddart, J. F. *J. Am. Chem. Soc.* **2004**, *126*, 2288–2289.

(12) (a) Beattie, D. R.; Hindmarsh, P.; Goodby, J. W.; Haslam, S. D.; Richardson, R. M. *J. Mater. Chem.* **1992**, *2*, 1261–1266. (b) Zniher, R.; Achour, R.; Cherkaoui, M. Z.; Donnio, B.; Gehringer, L.; Guillon, D. *J. Mater. Chem.* **2002**, *12*, 2208–2213.

(13) (a) Harger, M. J. P.; Westlake, S. *Tetrahedron* **1982**, *38*, 1511–1516. (b) Clive, D. L. J.; Kang, S. J. *J. Org. Chem.* **2001**, *66*, 6083–6091.

(14) (a) Boden, N.; Borner, R. C.; Bushby, R. J.; Cammidge, A. N.; Jesudason, M. V. *Liq. Cryst.* **1993**, *15*, 851–858. (b) Perez, D.; Guitián, E. *Chem. Soc. Rev.* **2004**, *33*, 274–283.

(15) (a) Markovitsi, D.; Germain, A.; Millié, P.; Lécuyer, P.; Gallos, L. K.; Argyrakos, P.; Bengs, H.; Ringsdorf, H. *J. Phys. Chem.* **1995**, *99*, 1005–1017, and references therein. (b) Balzani, V.; Clemente-León, M.; Credi, A.; Lowe, J. N.; Badjic, J. D.; Stoddart, J. F.; Williams, D. J. *Chem. Eur. J.* **2003**, *9*, 5348–5360. (c) Li, Z.; Lucas, N. T.; Wang, Z.; Zhu, D. *J. Org. Chem.* **2007**, *72*, 3917–3920.

(16) All measures were done with Mercury 1.4.2 program from Cambridge Crystallographic Data Centre, U.K. Macrae, C. F.; Edgington, P. R.; McCabe, P.; Pidcock, E.; Shields, G. P.; Taylor, R.; Towler, M.; van de Streek, J. *J. Appl. Crystallogr.* **2006**, *39*, 453–457.

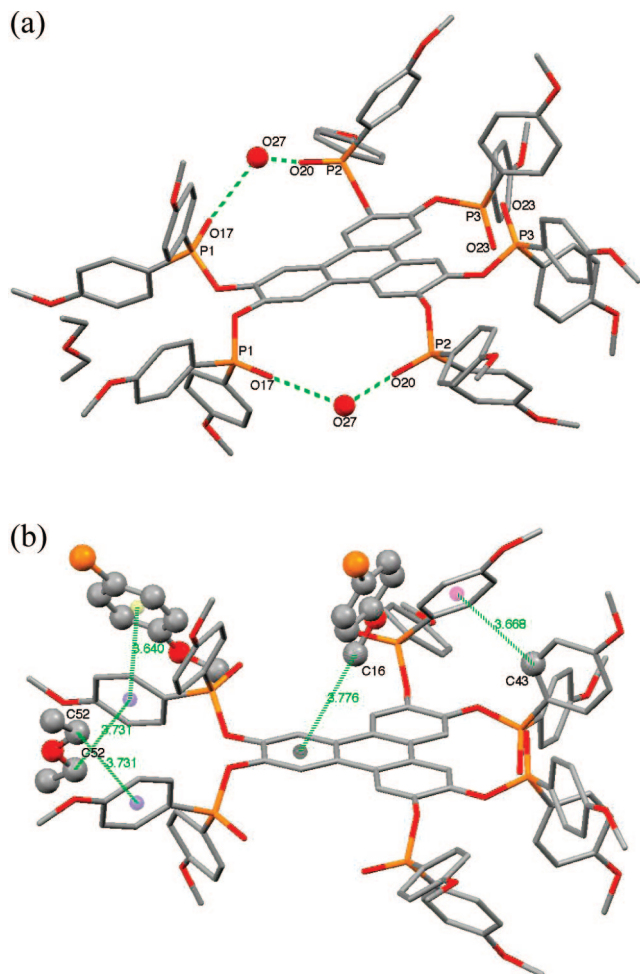


**FIGURE 2.** X-ray crystal structure of *Discopus 1b*·Et<sub>2</sub>O·2H<sub>2</sub>O. (a) One molecule of **1b**·Et<sub>2</sub>O·2H<sub>2</sub>O in stick representation. (b) View of intramolecular and intermolecular  $\pi$ - $\pi$  and CH- $\pi$  short contacts for one molecule of **1b** (capped stick). For clarity only partners moieties (ball and stick) are shown and interactions are indicated in green dotted lines.

**TABLE 1.** Hydrogen Bonds (D-H $\cdots$ A) Geometry: Distance (*d*, Å) and Angle ( $\langle$ DHA $\rangle$ , deg)

D-H <sup>a</sup>	P=A <sup>a</sup>	<i>d</i> (D-H)	<i>D</i> (H $\cdots$ A)	$\langle$ DHA $\rangle$	<i>d</i> (D $\cdots$ A)
O27-H27A	P2=O20	1.07(2)	1.75(2)	178.6(7)	2.811(3)
O27-H27B	P1=O17	0.99(2)	1.79(2)	172.4(8)	2.781(3)

<sup>a</sup> For atom numbering see Supporting Information.

whereas for P3=O this angle is 1.76° above the plane. Interestingly, positions of the six diarylphosphinate substituents are mainly governed by hydrogen bonds with water (involving four P=O groups, Figure 2a) and CH- $\pi$  short contacts (Figure 2b).

Indeed, two molecules of water are involved in cooperative hydrogen bonds with phosphinate groups (Figure 2a). Each water molecule is pinched between two phosphinate groups located in the same triphenylene bay region. Distances P=O $\cdots$ OH<sub>2</sub> $\cdots$ O=P are 2.78 and 2.81 Å, respectively, and H-bonding angles are closed to 180° (Table 1). These strong hydrogen bonds<sup>17</sup> are classical for phosphine oxide derivatives,<sup>18</sup> but to the best of our knowledge, these are the first example of a water molecule cooperative binder.

(17) Desiraju, G. R.; Steiner, T. In *The Weak Hydrogen Bond in Structural Chemistry and Biology*; Oxford University Press: New York, 1999.

In the crystal, *Discopus* molecules are located in parallel planes and their cores are distant by about 13.5 Å (intercores distances C5-C5 13.57 Å, C4-C4 13.01 Å, C7-C7 14.57 Å; see Supporting Information). From the Cambridge Structural Database, crystal structures of hexasubstituted triphenylenes,<sup>19</sup> which present no core  $\pi$ -stacking, have intermolecular cores distances ranging from 15.91 to 17.73 Å. Thus inter-*Discopus* distances are a little bit shorter as a result of  $\pi$ - $\pi$  and CH- $\pi$  short contacts between molecules. Indeed, two classical  $\pi$ -stackings were observed between *p*-methoxyphenyl groups: an intramolecular edge-to-face one between C43 and centroid C31-C36 (purple center in Figure 2b, 3.668 Å) as well as an intermolecular one between centroids C17-C22 and C31-C36 (respectively blue to yellow centers distance, 3.640 Å). Moreover, several intermolecular CH- $\pi$  short contacts were highlighted between *Discopus* and other molecules (Figure 2b and Supporting Information). A molecule of Et<sub>2</sub>O is pinched between two diarylphosphinate substituents as the distance between C52 (Et<sub>2</sub>O) and centroid C17-C22 (blue center in *Discopus*) is 3.731 Å. The triphenylene core is also close to a methoxy group from another *Discopus* molecule. The distance between centroid C7-C9 (black center) and C16 is 3.776 Å, which is typical of intermolecular CH- $\pi$  contacts (3.7-3.8 Å as found in proteins).<sup>20</sup> These multiple CH- $\pi$  contacts contribute to fulfill empty  $\pi$ -surfaces but cannot be interpreted as CH- $\pi$  interactions driving the crystal packing. In the literature, CH- $\pi$  contact examples involving triphenylenes are rare. Bushby et al. reported a crystal structure of an hepta-substituted triphenylene showing partial  $\pi$ -overlapping (C<sub>ar</sub> $\cdots$ C<sub>ar</sub> 3.72-3.79 Å) and also CH- $\pi$  contacts (C<sub>H</sub> $\cdots$ C<sub>ar</sub> 3.38-3.89 Å).<sup>19</sup> In the solid state, *Discopus 1b* was inclined to make hydrogen bonds along with CH- $\pi$  short contacts.

**Guest Affinities in Solution.** Proton NMR dilution experiments were conducted with compounds **1a,b** in chloroform. Critical aggregate concentrations were 6 mM for **1a** and 5 mM for **1b**. Titrations were thus achieved with a 1 mM host concentration. Phosphorus and proton NMR signals monitoring was carried out using *Discopus 1a,b* and model **3** (1 mM) in the presence of relevant guests **4** (0 to 10-25 mM). Sufficiently soluble in chloroform, targets **4** were chosen for their various electron-density or H-bonding abilities (Figure 1). Proton NMR observations were achieved on guest signals because changes in *Discopus* spectra were not significant.

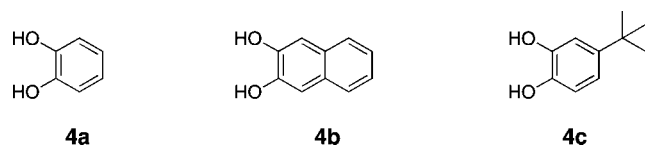
Electron-poor (1,3,5-trinitrobenzene) and unsubstituted aromatics (benzene, naphthalene), as well as electron-rich benzene derivatives (1,2-dimethoxybenzene, 1,3,5-trimethoxybenzene), showed no  $\pi$ - $\pi$  interaction with hosts **1a,b** and **3**. In contrast to polyaromatic-based tweezers,<sup>21</sup> *Discopus 1a,b* do not interact with electronic and size complementary aromatic compounds.

(18) Kariuki, B. M.; Harris, K. D. M.; Philp, D.; Robinson, J. M. A. *J. Am. Chem. Soc.* **1997**, *119*, 12679-12680.

(19) (a) Boden, N.; Bushby, R. J.; Jesudason, M. V.; Sheldrick, B. *Chem. Commun.* **1988**, 1342-1343. (b) Bushby, R. J.; Boden, N.; Kilner, C. A.; Lozman, O. R.; Lu, Z.; Liu, Q.; Thornton-Pett, M. A. *J. Mater. Chem.* **2003**, *13*, 470-474.

(20) (a) Nishio, M.; Hirota, M.; Umezawa, Y. In *The CH/π Interaction. Evidence, Nature and Consequences*; Wiley-VCH: New-York, 1998. (b) Takahashi, H.; Tsuboyama, S.; Umezawa, Y.; Honda, K.; Nishio, M. *Tetrahedron Lett.* **2000**, *56*, 6185-6191. (c) Takemura, H.; Iwanaga, T.; Shinmyozu, T. *Tetrahedron Lett.* **2005**, *46*, 6687-6690. (d) Brandl, M.; Weiss, M. S.; Jabs, A.; Sühnel, J.; Hilgenfeld, R. *J. Mol. Biol.* **2001**, *307*, 357-377.

(21) (a) Zimmerman, S. C.; Van Zyl, C. M.; Hamilton, G. S. *J. Am. Chem. Soc.* **1989**, *111*, 1373-1381, and references therein. (b) Klärner, F.-G.; Kahlert, B. *Acc. Chem. Res.* **2003**, *36*, 919-932. (c) Branchi, B.; Balzani, V.; Ceroni, P.; Campaña Kuchenbrandt, M.; Klärner, F.-G.; Bläser, D.; Boese, R. *J. Org. Chem.* **2008**, *73*, 5839-5851, and references therein.

**SCHEME 2. Structures of Catechols 4a–c That Form Host–Guest Complexes with *Discopus* 1a,b and Model 3**


In the presence of hydrogen bond donors, polyphosphinated hosts had uneven performance. A selective interaction appeared with 1,2-dihydroxybenzene (catechol) moieties (catechol **4a**, 1,2-dihydroxynaphthalene **4b**, and *tert*-butylcatechol **4c**, Scheme 2) and 1,3-dihydroxybenzene (resorcinol), but there was no binding with other aromatic hydrogen bond donors such as phenol derivatives (phenol, 1-hydroxy-2-methoxybenzene), aniline derivatives (aniline, 1,2-diaminobenzene, 1,3-diaminobenzene), and thiol derivatives (thiobenzene, 1,2-dithiobenzene).

These preliminary results suggested that one or more hydrogen bond(s) may exist between polyphosphinated *Discopus* and dihydroxybenzene derivatives. This weak interaction was not observed with phenols as the strength of hydrogen bonding is dependent upon donor–acceptor cooperativity and donor acidity, which follows the OH > NH > SH series.<sup>22</sup> Hydrogen bond strength is also depending on solvent polarity and might be absent in the presence of competing solvents.<sup>23</sup> Widely soluble, *Discopus* **1b** and guest **4b** associations were evaluated in organic solvents by the same protocol. In good hydrogen bond acceptor solvents (DMSO, acetone, and THF), guest **4b** was not complexed by the receptor. In non-competitive solvents (CHCl<sub>3</sub>, CH<sub>2</sub>Cl<sub>2</sub>, and acetonitrile), **1b**:**4b** association was present through significant NMR signal shifts. These observations are in accordance with hydrogen bonding between *Discopus* and catechol moieties.

To assess this point, we investigated the association between **1a,b** and **4a** by infrared spectroscopy. This technique also proved to be sensitive to hydrogen bonding involving P=O (or C=O) and phenol partners.<sup>24,25</sup>

**Infrared Studies.** As a preliminary study, infrared spectra of catechol **4a** were recorded to assign OH stretching and self-association bands (Figure 3). Compound **4a** exhibited two strong bands at 3600 and 3558 cm<sup>-1</sup>, with similar intensities in the OH stretching region.

The band observed at 3600 cm<sup>-1</sup> can be ascribed to the stretching vibration of free hydroxyl groups ( $\nu\text{OH}_f$ ), whereas the band at 3558 cm<sup>-1</sup> has been assigned to the stretching vibration of hydroxyl groups that formed intramolecular hydrogen bonds ( $\nu\text{OH}_{b \text{ intra}}$ ).<sup>26</sup>

As results for *Discopus* **1a** are similar (see Supporting Information), only the study of **1b** is reported. In CDCl<sub>3</sub>, the infrared spectra of receptor **1b** and catechol **4a**, as well as the mixture **1b**:**4a** in the 1:2 and 1:10 ratios, were recorded in

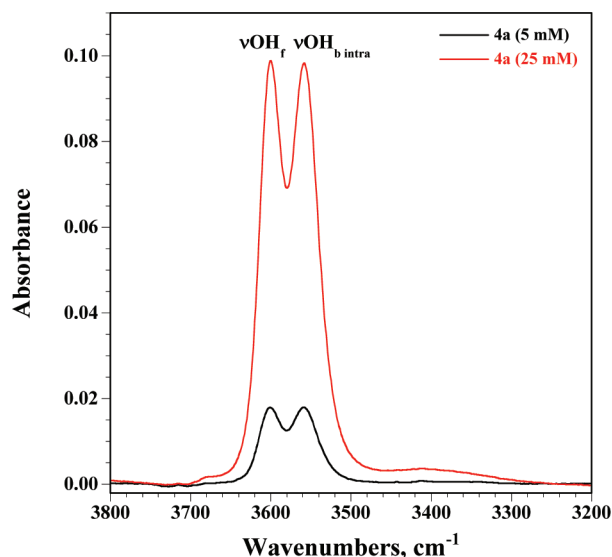


**FIGURE 3.** IR spectra (CDCl<sub>3</sub>) of catechol **4a** at concentrations of 5 mM (black line) and 25 mM (red line) in the 3800–3200 cm<sup>-1</sup> region.

the 3800–2600 cm<sup>-1</sup> (Figure 4a) and 1700–950 cm<sup>-1</sup> (Figure 4b) regions, respectively.

Spectrum of *Discopus* **1b** in the 3800–2600 cm<sup>-1</sup> region was essentially dominated by the aromatic and aliphatic C–H stretching vibrations. The IR spectrum for the mixture **1b**:**4a** in the 1:2 ratio was not the simple addition of the two spectra of **1b** (at a concentration of 2.5 mM) and **4a** (at a concentration of 5 mM), indicating that interactions occurred between the two molecules. A very broadband appears around 3200 cm<sup>-1</sup>, whereas the intensities of the two bands associated to the stretching vibrations of the free (at 3600 cm<sup>-1</sup>) and associated (at 3558 cm<sup>-1</sup>) hydroxyl groups decreased significantly. This behavior can be easily explained considering hydrogen bonds between catechol and receptor. The observed frequency around 3200 cm<sup>-1</sup> proved that weak hydrogen bonds occurred, as expected for phenols.<sup>27</sup> The intensity of the broadband was multiplied approximately by a factor 2 in the IR spectrum of **1b**:**4a** in the 1:10 ratio, which was consistent with a weak association constant between the two compounds. A broad shoulder appeared around 3380 cm<sup>-1</sup>, which was certainly associated to the  $\nu\text{OH}_{b \text{ inter}}$  mode of catechol.

The IR spectra recorded in the 1700–950 cm<sup>-1</sup> region (Figure 4b) for a mixture **1b**:**4a** in the 1:2 and 1:10 ratios were almost the addition of the two spectra of **1b** and **4a**, except in the 1240–1190 cm<sup>-1</sup> region where stretching vibration of the diarylphosphinate group (P=O) is expected.<sup>28</sup> Indeed, when the concentration of **4a** increased, the intensity of the band at 1228 cm<sup>-1</sup> decreased, whereas the intensity of the band at 1198 cm<sup>-1</sup> increased. This last band did not appear in the IR spectrum of **1b** and can be assigned to the stretching vibration of phosphinate groups involved in hydrogen bonds. The splitting between the stretching vibration of free (1228 cm<sup>-1</sup>) and associated (1198 cm<sup>-1</sup>) phosphinate groups were in agreement with those determined for hydrogen-bonded complexes between phenol and phosphoryl compounds.<sup>22</sup>

(22) (a) Abraham, M. H.; Grellier, P. L.; Prior, D. V.; Duce, P. P.; Morris, J. J.; Taylor, P. J. *J. Chem. Soc., Perkin Trans. II* **1989**, 699–711. (b) Abraham, M. H.; Duce, P. P.; Prior, D. V.; Barratt, D. G.; Morris, J. J.; Taylor, P. J. *J. Chem. Soc., Perkin Trans. II* **1989**, 1355–1375. (c) Abraham, M. H. *Chem. Soc. Rev.* **1993**, 73–83.

(23) Reichardt, C. In *Solvents and Solvent Effects in Organic Chemistry*, 2nd ed.; VCH: Weinheim, 1990.

(24) Modro, A. M.; Modro, T. A. *Can. J. Chem.* **1999**, *77*, 890–894.

(25) (a) Sijbesma, R. P.; Kentgens, A. P. M.; Lutz, E. T. G.; Van der Maas, J. H.; Nolte, R. J. M. *J. Am. Chem. Soc.* **1993**, *115*, 8999–9005. (b) Reek, J. N. H.; Priem, A. H.; Engelkamp, H.; Rowan, A. E.; Elemans, J. A. A. W.; Nolte, R. J. M. *J. Am. Chem. Soc.* **1997**, *119*, 9956–9964.

(26) Kjaergaard, H. G.; Howard, D. L.; Schofield, D. P.; Robinson, T. W.; Ishiuchi, S.; Fujii, M. *J. Phys. Chem. A* **2002**, *106*, 258–266.

(27) Novak, A. In *Structure and Bonding*; Dunitz, J. D., Hemmerich, P., Holm, R. H., Ibers, J. A., Jorgensen, C. K., Neilands, J. B., Reinen, D., Williams, R. J. P., Eds.; Springer-Verlag: Berlin, 1974; Vol. 18, pp 177–216.

(28) Socrates, G. In *Infrared Characteristic Group Frequencies*; Wiley Interscience: New York, 1980.

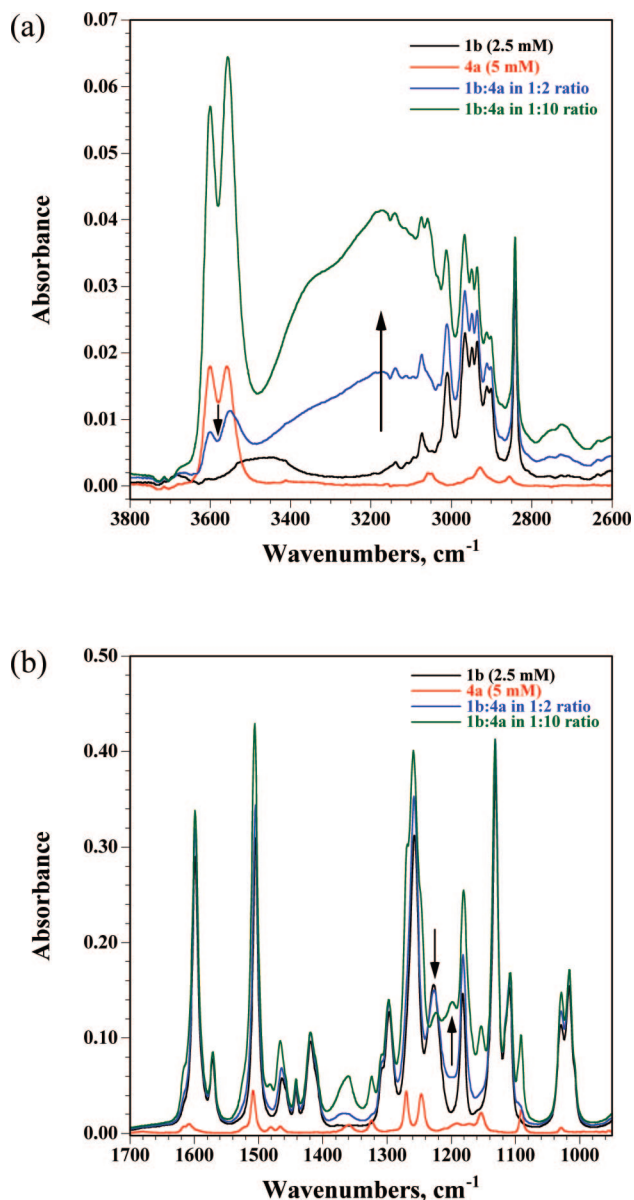


**FIGURE 4.** IR spectra ( $\text{CDCl}_3$ ) of *Discopus 1b* (black) and catechol **4a** (red), as well as the mixture **1:4a** in the 1:2 (blue) and 1:10 (green) ratios, recorded in (a) the 3800–2600  $\text{cm}^{-1}$  region and (b) the 1700–950  $\text{cm}^{-1}$  region.

Infrared studies undoubtedly proved that catechol **4a** makes hydrogen bonds with *Discopus*, especially with P=O acceptors, but other acceptors may participate in these weak associations.

**Binding Studies.** The quest for selective binding is one of the key issues in developing new molecular receptors. As previously observed, compounds **1a,b** showed affinity for catechol moieties versus phenol, aniline, and thiobenzene ones. Few examples of catechol receptors in chloroform have been reported.<sup>29,30</sup> Mainly based on carbonyl (ester, amide, urea) hydrogen bond acceptors, their associations with catechol derivatives were weak in chloroform, and association constants

(29) Catechol and dihydroxynaphthalene receptors in chloroform: (a) Sijbesma, R. P.; Nolte, R. J. M. *J. Org. Chem.* **1991**, *56*, 3122–3124. (b) Sijbesma, R. P.; Kentgens, A. P. M.; Nolte, R. J. M. *J. Org. Chem.* **1991**, *56*, 3199–3141. (c) Reference 25a. (d) Kawai, H.; Katoono, R.; Nishimura, K.; Matsuda, S.; Fujiwara, K.; Tsuji, T.; Suzuki, T. *J. Am. Chem. Soc.* **2004**, *126*, 5034–5035. (e) Cho, Y. L.; Uh, H.; Chang, S.-Y.; Chang, H.-Y.; Choi, M.-G.; Shin, I.; Jeong, K.-S. *J. Am. Chem. Soc.* **2001**, *123*, 1258–1259.

**TABLE 2.** Binding Constants of Phosphorylated Receptors **1a,b** and **3** toward Catechol Derivatives in  $\text{CDCl}_3$  at 298 K

guest	binding constants $K_{\text{ai}}$ ( $\text{M}^{-1}$ ) <sup>a,b</sup>		
	model <b>3</b>	<i>Discopus 1a</i>	<i>Discopus 1b</i>
<b>4a</b>	92 (88) <sup>c</sup>	1407; 70 (109) <sup>c</sup>	2834; 85 (84) <sup>c</sup> 2949; <sup>d</sup> 73 <sup>d</sup>
<b>4b</b>	n.d.	1441; 30 (51) <sup>c</sup>	1863; 97 (114) <sup>c</sup> 1887; <sup>d</sup> 189 <sup>d</sup>
<b>4c</b>	n.d.	n.d.	144; 67 (65) <sup>c</sup>

<sup>a</sup> Monitoring guest protons by NMR. <sup>b</sup> Experiments were run twice at least and  $\pm 15\%$  errors were estimated. <sup>c</sup> From  $^{31}\text{P}$  NMR titration. <sup>d</sup> From microcalorimetric titration with  $\pm 5\%$  errors.

( $K_a$ ) ranged from 14 to 120  $\text{M}^{-1}$ . In the same solvent, curved receptors for resorcinol derivatives or dihydroxynaphthalenes proved to be more efficient ( $K_a$  from 30 to  $1 \times 10^{+5}$   $\text{M}^{-1}$ ), using cooperative hydrogen bonds and eventually additional  $\pi$ – $\pi$  stacking.<sup>31</sup> To quantify binding properties of receptors **1a,b** and **3**, Job plots and titrations toward catechols **4a–c** were performed in  $\text{CDCl}_3$  using  $^1\text{H}$  and  $^{31}\text{P}$  NMR monitoring (Table 2).<sup>32,33</sup>

Both  $^1\text{H}$  and  $^{31}\text{P}$  NMR titrations demonstrated that model **3** forms a 1:1 complex with guest **4a** whose association constant is  $90 \pm 2$   $\text{M}^{-1}$ . Infrared study in  $\text{CDCl}_3$  showed that catechol function was involved in binding (decreasing intensity around 3600  $\text{cm}^{-1}$  and increasing intensity around 3200  $\text{cm}^{-1}$ ), but no evidence of P=O implication was seen in the 1240–1190  $\text{cm}^{-1}$  region due to signal overlap (see Supporting Information). Nevertheless,  $^{31}\text{P}$  NMR proved to be sensitive to this association, which probably is hydrogen bonding between host phosphinates and guest catechol function. As expected, both *Discopus* structures had recognition properties different from those of **3** (Figure 5).

Interestingly, *Discopus 1a,b* are associated to target **4a** in a 1:2 (host:guest) complex allowing  $^1\text{H}$  NMR monitoring (Table 2). The corresponding association constants  $K_{a1}$  and  $K_{a2}$  are 1407 and 70  $\text{M}^{-1}$  for **1a** and slightly higher for **1b**, 2834  $\text{M}^{-1}$  and 85  $\text{M}^{-1}$ , respectively. A first catechol is thus strongly recognized by *Discopus 1a,b* and a second catechol is complexed as weakly as in the case of host **3**. Moreover, the second association is also observed by  $^{31}\text{P}$  NMR titrations (1:1 complex, confirming  $K_{a2}$  values). Only the second catechol binding site ( $K_{a2}$ ) involves phosphinate groups as probably hydrogen bond acceptors. Hence *Discopus 1a,b* are ditopic receptors for catechol **4a** which was confirmed by microcalorimetric titrations with **1b** (sequential binding model, see Supporting Information). Concerning the better binding ability of **1b** compared to **1a**, methoxy substituents in **1b** might offer potent hydrogen bonds acceptors sites to **4a**.

(30) Catechol receptors in aqueous medium: (a) Wiskur, S. L.; Lavigne, J. J.; Metzger, A.; Tobey, S. L.; Lynch, V.; Anslын, E. V. *Chem. Eur. J.* **2004**, *10*, 3792–3804. (b) Diaz, S. G.; Lynch, V.; Anslын, E. V. *J. Supramol. Chem.* **2002**, *2*, 201–209. (c) Imada, T.; Kijima, H.; Takeuchi, M.; Shinkai, S. *Tetrahedron* **1996**, *52*, 2817–2826. (d) Bernardo, A. R.; Stoddart, J. F.; Kaifer, A. E. *J. Am. Chem. Soc.* **1992**, *114*, 10624–10631. (e) Kimura, E.; Watanabe, A.; Kodama, M. *J. Am. Chem. Soc.* **1983**, *105*, 2063–2066.

(31) Resorcinol and phenols recognition in organic solvents: (a) Murray, B. A.; Whelan, G. S. *Pure Appl. Chem.* **1996**, *68*, 1561–1567. (b) Mirzoiyan, A.; Kaifer, A. E. *J. Org. Chem.* **1995**, *60*, 8093–8095. (c) Reference 25b.

(32) NMR titrations were fitted using HypNMR2006, a commercial program from Protonic Software. Frassinetti, C.; Ghetti, S.; Gans, P.; Sabatini, A.; Moruzzi, M. S.; Vacca, A. *Anal. Biochem.* **1995**, *231*, 374–382.

(33) NMR titrations were also run between *Discopus 1b* and resorcinol. Proton NMR data were fitted with a (1:2) complex whose association constants were  $K_{a1} = 687$   $\text{M}^{-1}$  and  $K_{a2} = 100$   $\text{M}^{-1}$ . Phosphorus NMR data could not be fitted in model (1:1) or (1:2) with sufficient confidence. In the case of resorcinol, phosphinates groups involvement in recognition is more complex than in **1b:4a** complexes.

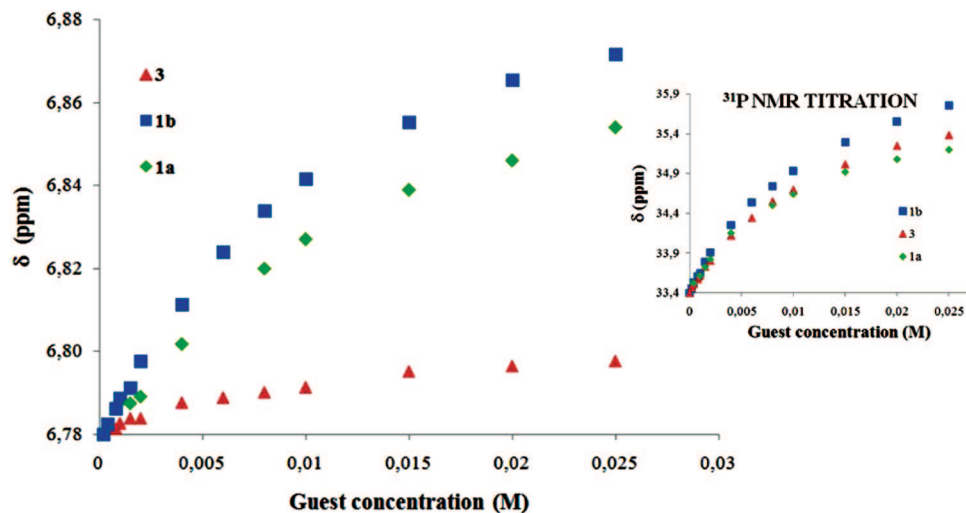


**FIGURE 5.**  $^1\text{H}$  NMR titrations of hosts **1a** (green diamonds), **1b** (blue squares), and **3** (red triangles) toward catechol **4a** (0–25 mM,  $\text{CDCl}_3$ ). Inset:  $^{31}\text{P}$  NMR titrations of receptors **1a,b** and **3** toward **4a**.

Catechol **4b** was also recognized by *Discopus* **1a,b** with the same 1:2 (host:guest) stoichiometry as **4a**. Again, *Discopus* **1b** was a better ligand than **1a**. On one hand, guest **4b** had similar association constants ( $K_{a1} = 1441 \text{ M}^{-1}$  and  $K_{a2} = 30 \text{ M}^{-1}$ ) as **4a** with **1a**, and on the other hand, guest **4b** was less associated ( $K_{a1} = 1863 \text{ M}^{-1}$  and  $K_{a2} = 97 \text{ M}^{-1}$ ) than **4a** with **1b** (confirmed by microcalorimetric titrations). In all cases, *Discopus* **1b** was the best receptor.

To explain the stronger  $K_{a1}$  values compared to the  $K_{a2}$  ones, we speculated that hydrogen bonding could occur with oxygens located at the triphenylene periphery and thus it could benefit from supplementary  $\pi-\pi$  interaction between the receptor large  $\pi$ -core and catechol. Bulky guest **4c** was titrated by *Discopus* **1b** in order to evaluate the effect of steric hindrance while OH functions are available for binding. From NMR titrations, target **4c** forms 1:2 (host:guest) complex with **1b**, as observed for **4a,b** compounds, but association constants were lower than those measured between **4a,b** and the same host (Table 2).  $K_{a1}$  dramatically decreased to  $144 \text{ M}^{-1}$ , while  $K_{a2}$  was slightly lower ( $65 \text{ M}^{-1}$ ). Thus steric hindrance disordered the first step of complexation while the second step ( $\text{P}=\text{O}\cdots\text{H}-\text{OAr}$  hydrogen bond) was just affected by electronic effect. These observations are in accordance with the hypothesis that the first adduct may rely on an H-bond assisted by  $\pi-\pi$  interaction.

Further investigation was undertaken with molecular modeling to elucidate binding sites within the 1:2 association.

**Molecular Dynamics Simulations.** Molecular dynamics (MD) involves the simulation of the dynamic motions of the complex atoms using the differential equations of motion with the molecular mechanics CVFF force field through a series of infinitesimal time increments. A molecular modeling study was carried out to model a 3D structure of **3:4a** and **1b:4a** complexes and to get insight into major molecular interactions. A geometry optimization of each complex was followed by MD simulations.

During MD simulation, model **3** had several types of hydrogen bonds with catechol **4a**. Hydrogen bonding acceptors were mainly phosphinate groups  $\text{P}=\text{O}$ , triphenylene out-rim oxygens, and to a less extent, arylmethoxy oxygens (Figure 6). These weak interactions could be multiple within the complex (Figure 6b). This modeling is in agreement with experimental observations using NMR and infrared spectroscopies.

Concerning the MD simulation of **1b** in the presence of two molecules **4a**, it is noteworthy that one catechol remains over

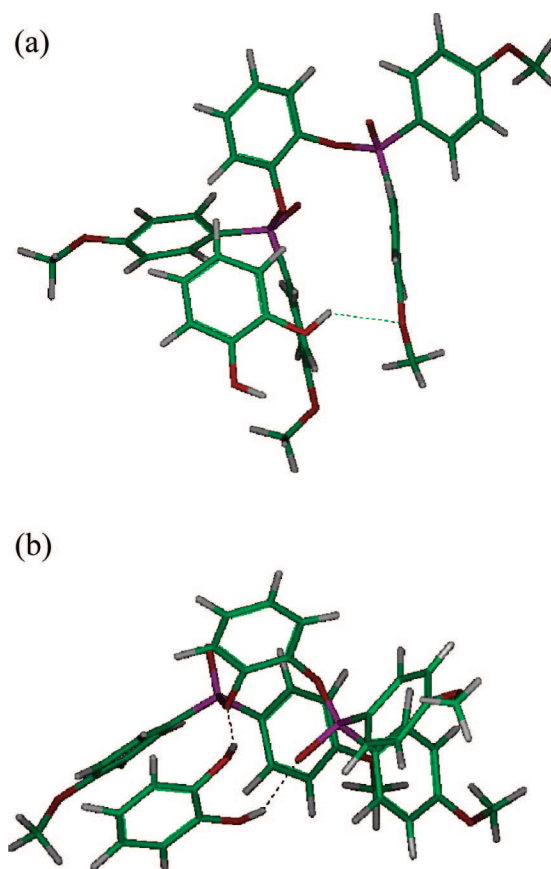


**FIGURE 6.** Snapshots of MD simulation between model **3** and **4a**. (a) Aryl methoxy oxygen atom as hydrogen bond acceptor. (b) Phosphinate groups and triphenylene-linked oxygen atoms as hydrogen bond acceptor.

the triphenylene core of *Discopus* **1b** as a result of  $\pi-\pi$  stacking, as the distance between aromatic moieties is about  $3.57 \text{ \AA}$  (Figure 7). This catechol is also involved in a hydrogen bond network with three different oxygen atoms ( $\text{P}=\text{O}$ ,  $\text{OMe}$ , and triphenylene-linked oxygens) (see Supporting Information). Additional interaction between catechol and methoxy groups with complex **1b:4a** may explain that, experimentally, *Discopus* **1b** is a better ligand than **1a**, which is not fitted with OMe substituents.

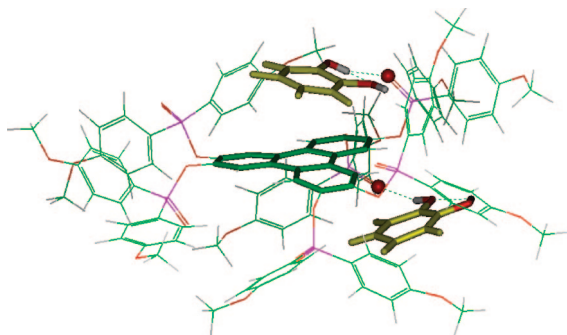


**FIGURE 7.** Snapshot of MD simulation where two guests **4a** (in yellow) make hydrogen bonds with phosphinate groups and  $\pi$ - $\pi$  interactions with the triphenylene core of *Discopus 1b*.

The MD experiment also showed that the second **4a** compound moved outside the polyaromatic core, establishing hydrogen bonds with P=O moieties and triphenylene-linked oxygens. These intermolecular hydrogen bonds were conserved during the dynamics, although the phosphinate groups involved are different. Moreover, the dynamics simulation revealed that intramolecular hydrogen bonds between hydroxyl groups of **4a** occurred frequently.

Hence, MD simulations for complex **1b:4a** (in a 1:2 ratio) corroborate experiments, showing that *Discopus* makes multiple hydrogen bonds with **4a** within two distinct binding sites. One catechol makes hydrogen bonds at the *Discopus* periphery, whereas the other one is located above triphenylene core as a result of hydrogen bonds and  $\pi$ -interaction. Nevertheless, MD predicted that both catechol molecules may interact with P=O groups, which is in contradiction with experience:  $^{31}\text{P}$  NMR proved that only one molecule of **4a** was complexed by phosphinate functions.

Modeling and spectroscopic experiments were thus complementary to establish the structure of *Discopus*-catechol associations.

## Conclusion

In summary, we have demonstrated that *Discopus 1a,b* can be easily prepared in efficient overall yields. X-ray analysis revealed that conformation of **1b**, in the solid state, is governed by P=O H-bonding to water and intermolecular CH- $\pi$  short contacts. In chloroform solution, these unpreorganized receptors selectively interact with catechol guests in a 1:2 (host:guest) stoichiometry. *Discopus 1a,b* also proved to be ditopic, allowing distinct hydrogen bonds with, on one hand, classical phosphinate group acceptors, as observed by infrared spectroscopy, and on the other hand, a stronger H-bond assisted by  $\pi$ -interaction with triphenylene core, relying on MD simulations. As selective catechol receptors are needed, efforts are undertaken toward modified phosphinated *Discopus* to enhance association constants.

## Experimental Section

Compound **2** was prepared from commercial veratrole according to literature procedures.<sup>12</sup>

**Bis(4-methoxyphenyl) Phosphoric Acid Chloride.**<sup>13</sup> To a suspension of commercial bis(4-methoxyphenyl) phosphoric acid (5 g, 18 mmol) in dry dichloromethane (100 mL) at 0 °C was added dropwise oxalyl chloride (9 mL, 45 mmol) under inert conditions. The mixture was stirred at 0 °C for 20 min and at room temperature overnight. The crude liquid was concentrated under reduced pressure. Dry dichloromethane (100 mL) was added and evaporated

in vacuo to remove oxalyl chloride excess (repeated three times). The residual yellow oil (5.340 g, 99%) was used without further purification:  $^1\text{H}$  NMR (300 MHz,  $\text{CDCl}_3$ , 295 K)  $\delta$  7.76 ppm (dd,  $^3J_{\text{HH}} = 8.7$  Hz,  $^3J_{\text{PH}} = 12.3$  Hz, 4H,  $\text{H}_2$ ), 6.98 (dd,  $^3J_{\text{HH}} = 8.7$  Hz,  $^4J_{\text{PH}} = 3.4$  Hz, 4H,  $\text{H}_3$ ), 3.83 (s, 6H,  $\text{H}_5$ );  $^{13}\text{C}$  NMR (75.5 MHz,  $\text{CDCl}_3$ , 295 K)  $\delta$  163.3 (d,  $^4J_{\text{PC}} = 3.3$  Hz,  $\text{C}_4$ ), 133.0 (d,  $^2J_{\text{PC}} = 13.2$  Hz,  $\text{C}_2$ ), 124.6 (d,  $^1J_{\text{PC}} = 131.2$  Hz,  $\text{C}_1$ ), 114.2 (d,  $^3J_{\text{PC}} = 15.9$  Hz,  $\text{C}_3$ ), 55.5 ( $\text{C}_5$ );  $^{31}\text{P}$  NMR (120 MHz,  $\text{CDCl}_3$ , 295 K)  $\delta$  45.6 ppm (s).

**2,3,6,7,10,11-Hexa(diphenylphosphinate)triphenylene 1a.** To a solution of 2,3,6,7,10,11-hexahydroxytriphenylene **2** (0.649 g, 2 mmol) and triethylamine (8 mL, 20 mmol) in dry tetrahydrofuran (100 mL) at 0 °C was added dropwise a solution of diphenylphosphoric acid chloride (3.90 mL, 20 mmol) in dry tetrahydrofuran (10 mL). The reaction mixture was stirred at reflux overnight. Distilled water (200 mL) and dichloromethane (150 mL) were added at room temperature. After decantation, the aqueous phase was extracted with dichloromethane (2  $\times$  200 mL). The combined organic phases were washed with distilled water (2  $\times$  400 mL) and brine (2  $\times$  300 mL), dried over magnesium sulfate, filtered, and concentrated in vacuo. The beige foam was suspended in hot dichloromethane (100 mL), filtered, and washed with dichloromethane (3  $\times$  5 mL). The filtrate was concentrated in vacuo and submitted to the same suspension-washing process twice. After column chromatography (dichloromethane/tetrahydrofuran 85:15), compound **1a** was isolated as a white solid (1.921 g, 63% yield):  $R_f$  0.24 (dichloromethane/tetrahydrofuran 85:15); mp 160 °C (dec); IR (NaCl)  $\nu$  3004, 2856, 1593, 1503, 1465, 1419, 1210, 1126, 1002  $\text{cm}^{-1}$ ; UV-vis ( $\text{CHCl}_3$ ,  $5 \times 10^{-6}$  M)  $\lambda_{\text{max}}$  ( $\epsilon$ ) 319 (9360), 299 (24650), 274 (119794), 266 (89255), 249 nm (34800  $\text{mol}^{-1} \text{L cm}^{-1}$ );  $^1\text{H}$  NMR (300 MHz,  $\text{CDCl}_3$ , 295 K)  $\delta$  8.12 (s, 6H,  $\text{H}_b$ ), 7.48–7.94 (dd,  $^3J_{\text{HH}} = 8.3$  Hz,  $^3J_{\text{PH}} = 12.5$  Hz, 24H,  $\text{H}_e$ ), 7.33 (m, 36H,  $\text{H}_f$  and  $\text{H}_g$ );  $^{13}\text{C}$  NMR (75.5 MHz,  $\text{CDCl}_3$ , 295 K)  $\delta$  141.8 (d,  $^2J_{\text{PC}} = 6.04$  Hz,  $\text{C}_e$ ), 132.6 (d,  $\text{C}_g$ ), 132.0 (d,  $^2J_{\text{PC}} = 10.6$  Hz,  $\text{C}_e$ ), 130.3 (d,  $^1J_{\text{PC}} = 137.0$  Hz,  $\text{C}_d$ ), 128.7 (d,  $^3J_{\text{PC}} = 13.6$  Hz,  $\text{C}_f$ ), 125.9 ( $\text{C}_a$ ), 116.0 ( $\text{C}_b$ );  $^{31}\text{P}$  NMR (120 MHz,  $\text{CDCl}_3$ , 295 K)  $\delta$  32.53 (s); LRMS (LSIMS)  $m/z$  (%) 1525 (35,  $[\text{M} + \text{H}]^+$ ), 1547 (100,  $[\text{M} + \text{Na}]^+$ ); HRMS (LSIMS)  $m/z$  calcd for  $\text{C}_{90}\text{H}_{66}\text{O}_{12}\text{P}_6\text{Na}$  ( $[\text{M} + \text{Na}]^+$ ) 1547.282722, found 1547.287760.

**2,3,6,7,10,11-Hexa(bis(4-methoxyphenyl)phosphinate)triphenylene 1b.** To a solution of compound **2** (0.649 g, 2 mmol) and triethylamine (8 mL, 20 mmol) in dry tetrahydrofuran (100 mL) at 0 °C was added dropwise a solution of freshly prepared bis-(4-methoxyphenyl) phosphoric acid chloride (5.340 g, 18 mmol) in tetrahydrofuran (10 mL). The reaction mixture was stirred at room temperature overnight. Distilled water (100 mL) and dichloromethane (150 mL) were added. After decantation, the aqueous phase was extracted with dichloromethane (2  $\times$  200 mL). The combined organic phases were washed with distilled water (2  $\times$  400 mL) and brine (2  $\times$  300 mL), dried over magnesium sulfate, filtered, and concentrated in vacuo. The beige foam was dissolved with ethyl acetate (200 mL). After precipitation, the suspension was filtered and dried under vacuum. Compound **1b** was isolated as a white solid (2.305 g, 61%):  $R_f$  0.23 (dichloromethane/tetrahydrofuran 8:2); mp 156 °C (dec); IR (NaCl)  $\nu$  2972, 2836, 1589, 1513, 1454, 1418, 1255, 1137, 1013  $\text{cm}^{-1}$ ; UV-vis ( $\text{CHCl}_3$ ,  $5 \times 10^{-6}$  M)  $\lambda_{\text{max}}$  ( $\epsilon$ ) 319 (9360), 299 (24278), 274 (136653), 264 (124812), 249 nm (154089  $\text{mol}^{-1} \text{L cm}^{-1}$ );  $^1\text{H}$  NMR (300 MHz,  $\text{CDCl}_3$ , 295 K)  $\delta$  8.06 (s, 6H,  $\text{H}_b$ ), 7.87 (dd,  $^3J_{\text{HH}} = 8.7$  Hz,  $^3J_{\text{PH}} = 12.3$  Hz, 24H,  $\text{H}_e$ ), 6.89 (dd,  $^3J_{\text{HH}} = 8.7$  Hz,  $^4J_{\text{PH}} = 2.7$  Hz, 24H,  $\text{H}_f$ ), 3.79 (s, 36H,  $\text{H}_h$ );  $^{13}\text{C}$  NMR (75.5 MHz,  $\text{CDCl}_3$ , 295 K)  $\delta$  162.7 (d,  $^4J_{\text{PC}} = 3.02$  Hz,  $\text{C}_g$ ), 141.8 ( $\text{C}_e$ ), 133.9 (d,  $^2J_{\text{PC}} = 12.1$  Hz,  $\text{C}_e$ ), 125.8 ( $\text{C}_a$ ), 121.9 (d,  $^1J_{\text{PC}} = 145.7$  Hz,  $\text{C}_d$ ), 116.0 ( $\text{C}_b$ ), 114.2 (d,  $^3J_{\text{PC}} = 14.8$  Hz,  $\text{C}_f$ ), 55.2 ( $\text{C}_h$ );  $^{31}\text{P}$  NMR (120 MHz,  $\text{CDCl}_3$ , 295 K)  $\delta$  33.28 (s); LRMS (MALDI)  $m/z$  (%) 1885 (60,  $[\text{M} + \text{H}]^+$ ), 1908 (100,  $[\text{M} + \text{Na}]^+$ ); HRMS (LSIMS)  $m/z$  calcd for  $\text{C}_{102}\text{H}_{90}\text{O}_{24}\text{P}_6$  ( $[\text{M} + \text{H}]^+$ ) 1885.438065, found 1885.432610.

**1,2-Di(bis(dimethoxyphenyl)phosphinate)benzene 3.** The same procedure as for *Discopus 1a* synthesis was followed using a

solution of catechol (220.2 mg, 2 mmol) and triethylamine (840  $\mu\text{L}$ , 6.2 mmol) in dry THF (40 mL) and a solution of freshly prepared bis(4-methoxyphenyl) phosphoric acid chloride (1.828 g, 6.2 mmol) in dry THF (3 mL). After reaction and extraction, the crude product was column chromatographed on silica gel (ethyl acetate/petroleum ether 9:1) and compound **3** was isolated as a white solid (756 mg, 60%);  $R_f = 0.25$  (ethylacetate/petroleum ether 9:1); mp 72–74 °C (dec); IR (NaCl)  $\nu$  2932, 2840, 1597, 1502, 1454, 1409, 1230, 1129, 1025  $\text{cm}^{-1}$ ; UV–vis ( $\text{CHCl}_3$ ,  $1.3 \times 10^{-5}$  M)  $\lambda_{\text{max}}$  ( $\epsilon$ ) 280 (3932), 247 (43707), 240 nm (40098  $\text{mol}^{-1} \text{L cm}^{-1}$ );  $^1\text{H NMR}$  (250.13 MHz,  $\text{CDCl}_3$ , 295 K)  $\delta$  7.78 (dd,  $^3J_{\text{HH}} = 8.7$  Hz,  $^3J_{\text{PH}} = 12.1$  Hz, 8H,  $\text{H}_c$ ), 7.32 (m, 2H,  $\text{H}_b$ ), 6.87 (dd,  $^3J_{\text{HH}} = 8.9$  Hz,  $^4J_{\text{PH}} = 2.8$  Hz, 10H,  $\text{H}_f$  and  $\text{H}_a$ ), 3.81 (s, 12H,  $\text{H}_h$ );  $^{13}\text{C NMR}$  (62.9 MHz,  $\text{CDCl}_3$ , 295 K)  $\delta$  162.76 (d,  $^4J_{\text{PC}} = 2.9$  Hz,  $\text{C}_g$ ), 141.07 (d,  $^2J_{\text{PC}} = 7.6$  Hz,  $\text{C}_c$ ), 133.78 (d,  $^2J_{\text{PC}} = 12.4$  Hz,  $\text{C}_e$ ), 124.71 ( $\text{C}_a$ ), 122.37 (d,  $^1J_{\text{PC}} = 145.9$  Hz,  $\text{C}_d$ ), 121.61 (d,  $^3J_{\text{PC}} = 3.8$  Hz,  $\text{C}_b$ ), 114.12 (d,  $^3J_{\text{PC}} = 14.3$  Hz,  $\text{C}_f$ ), 55.33 ( $\text{C}_h$ );  $^{31}\text{P NMR}$  (120.1 MHz,  $\text{CDCl}_3$ , 295 K)  $\delta$  32.76 (s); LRMS (MALDI)  $m/z$  (%) 631 (90,  $[\text{M} + \text{H}]^+$ ), 653 (10,  $[\text{M} + \text{Na}]^+$ ); HRMS (LSIMS)  $m/z$  calcd for  $\text{C}_{102}\text{H}_{90}\text{O}_{24}\text{P}_6$  653.14784, found 653.14647.

**X-ray Crystallographic Data for *Discopus 1b*·Et<sub>2</sub>O·2H<sub>2</sub>O.** A crystal of  $0.5 \times 0.2 \times 0.1$  mm<sup>3</sup> approximate dimensions was mounted in a loop with mineral oil and transferred immediately in a nitrogen cold gas stream for flash cooling. The data were collected at 100 K with a Bruker SMART 6000 CCD area-detector diffractometer using Cu K $\alpha$  ( $\lambda = 1.54178$  Å) radiation. The unit cell parameters were refined using all the collected spots after the integration process. The redundancy in data allowed a semiempirical absorption correction (SADABS version 2.03)<sup>34</sup> to be applied on the basis of multiple measurements of equivalent reflections. Data reduction was accomplished with SAINT version 6.02a.<sup>34</sup> The structure was solved by direct methods and refined by full-matrix least-squares on  $F^2$  using SHELXL97.<sup>35</sup> All non-hydrogen atoms were refined with anisotropic temperature factors. The hydrogen atoms of the water molecule were localized by Fourier difference. The other hydrogen atoms were calculated with AFIX and included in the refinement with a common isotropic temperature factor. They were allowed to ride on their parent atoms.

Crystal data for **1b**·Et<sub>2</sub>O·2H<sub>2</sub>O: monoclinic, space group  $C2/c$ ,  $a = 25.4815(8)$ ,  $b = 21.1342(8)$ ,  $c = 19.4278(7)$  Å,  $\beta = 111.556(3)^\circ$ ,  $V = 9730.6$  Å<sup>3</sup>,  $Z = 4$ ,  $D_x = 1.36$  g  $\text{cm}^{-3}$ , 48318 total reflections collected, 9212 independent reflections of which 7667 were considered as observed ( $I > 2\sigma(I)$ ). Data were collected up to  $2\theta_{\text{max}} = 144^\circ$ , completeness 96.5%, 640 parameters,  $R_1 = 0.049$ ,  $wR_2 = 0.1273$ ,  $S = 1.027$ . Largest peak and hole in final residual electron density: 0.675 and  $-0.379$  e Å<sup>-3</sup>. Selected distances in *Discopus 1b* crystal are reported in Supporting Information. CCDC-685480 contains the supplementary crystallographic data for this paper. These data can be obtained free of charge from The Cambridge Crystallographic Data Centre via [www.ccdc.cam.ac.uk/data\\_request/cif](http://www.ccdc.cam.ac.uk/data_request/cif).

**FTIR Measurements.** Infrared spectra of *Discopus 1a,b* and catechol **4a**, as well as a mixture of **1a** (or **1b**) + **4a**, were recorded with a ThermoNicolet Nexus 670 FTIR spectrometer at a resolution of 4  $\text{cm}^{-1}$ , by coadding 50 scans. Samples were held in a variable path length cell with BaF<sub>2</sub> windows. Each spectra of **1a**, **1b**, and **4a** were measured in  $\text{CDCl}_3$  at a concentration of 2.5 mM and at a path length of 250  $\mu\text{m}$ . Additional spectra of **4a** were run at concentrations of 5 and 25 mM. Spectra of **1a** (or **1b**) + **4a** were measured in a 1:2 and 1:10 molar ratios. All infrared spectra are shown with solvent absorption subtracted out.

**Molecular Modeling.** The molecular structure of catechol **4a** was built with AMPAC 8.16. A geometry optimization was performed using the AM1 Hamiltonian, and the resulting catechol structure

was added to the X-ray structure of *Discopus 1b*. The **3:4a** (1:1 ratio) and **1b:4a** (1:2 ratio) structures were subjected to energy minimization using steepest descent followed by a conjugated gradient until the rms gradient was less than 0.001 kcal  $\text{mol}^{-1}$  Å<sup>-1</sup>. The consistent valence force field (CVFF) in the Discover molecular mechanics module of InsightII (Accelrys Inc.) was chosen for the evaluation of the potential energy function and atom typing due to its applicability in handling a wide range of organic systems. Cross-terms were used in the energy expression and a Morse potential was used to model the valence bond stretching term. Molecular dynamics simulations were performed with a target temperature of 300 K reached in 20 000 fs (equilibration), while the time step was 1.5 fs. The simulations were carried out using the Verlet leapfrog algorithm<sup>36</sup> and the structures were stored in the computer every 0.5 ps. Molecular dynamics was monitored during 750 ps. All simulations and visualization were performed with InsightII on a SGI Octane computer.

**NMR Titrations.** NMR signal monitoring was conducted on hosts **1a,b** and **3** ( $^{31}\text{P}$  singlet) as well as guests **4a–c** (protons). All solutions were freshly prepared, and deuterated solvents were dried over molecular sieves. A solution (250  $\mu\text{L}$ ) of host ( $\sim 2$  mM) was introduced in each NMR tube (12–15 experiments per titration). Increasing aliquots of guest stock solution ( $\sim 50$  mM) were added, and the total volume (500  $\mu\text{L}$ ) was adjusted with  $\text{CDCl}_3$ . The titration data ( $\Delta\delta$  ppm versus guest or host concentration) were fitted using the nonlinear curve-fitting procedure with either a (1:1) binding equation developed by Wilcox<sup>37</sup> using Origin 7.0 software or a (1:2) model using HypNMR2006 program.

**Microcalorimetric Titrations.** Isothermal titration calorimetry (ITC) experiments were conducted at 295 K in chloroform to allow a direct comparison with NMR studies. Host **1b** and guest solutions **4a** or **4b** were freshly prepared using HPLC grade solvent dried over molecular sieves. Stock host solution (0.742 mM,  $\text{CHCl}_3$ ) was placed into ITC cell ( $V = 1.4192$  mL). Aliquots (4  $\mu\text{L}$ ) of guest solution ( $\sim 30$  mM) were added via a computer-automated injector at 135 s intervals. Heat changes were recorded after each addition. Heats of dilution were measured by a blank experiment (in absence of receptor) under the same conditions and they were subtracted from the titration data prior to curve fitting. Additionally, an initial 2  $\mu\text{L}$  injection was discarded from each data set in order to remove the effect of titrant diffusion across the syringe tip during the equilibration process. Titrations curves were fitting with the sequential binding sites model (with two nonidentical binding sites) using Origin v. 5.0 software. Experiments were duplicated at least and data were averaged to be compared to NMR results.

**Acknowledgment.** This work was supported by the French Ministry of Research (C.G. Fellowship) and the Centre National de la Recherche Française. The authors thank Dr. Clarisse Maechling from the Faculté de Pharmacie de Strasbourg, Illkirch (France) for helping C.G. in the microcalorimetry experiments.

**Supporting Information Available:** Additional distances and views of crystal **1b**·Et<sub>2</sub>O·2H<sub>2</sub>O; snapshots of MD simulations for **3:4a** and **1b:4** complexes; UV–vis absorption and NMR spectra of compounds **1a,b** and **3**; FTIR spectra of **3** + **4a** and **1b** + **4a** mixtures; microcalorimetric titrations of **1b** toward **4a,b**; Job plots,  $^1\text{H}$  and  $^{31}\text{P}$  NMR titrations of hosts **1a,b** and **3** toward guests **4a–c**; and a cif file containing crystallographic data for **1b**·Et<sub>2</sub>O·2H<sub>2</sub>O. This material is available free of charge via the Internet at <http://pubs.acs.org>.

JO802015K

(34) Bruker, SMART, SADBS and SAINT; Bruker AXS Inc.: Madison, WI, 1997.

(35) Sheldrick, G. M. SHELXS-97 and SHELXL-97, Program for Crystal Structure Refinement; University of Göttingen:Göttingen, Germany, 1997.

(36) Verlet, L. *Phys. Rev.* **1967**, *159*, 98–103.

(37) Wilcox, C. S. In *Frontiers in Supramolecular Organic Chemistry and Photochemistry*; Schneider, H.-J., Dürr, H., Eds; VCH-Weinheim: Weinheim, Germany, 1991; pp 123–143.